Liquid Argon - Based Antineutrino Detection Techniques for Nuclear Waste Verification

Mădălina Wittel[1]
Malte Göttsche[1,2]
Achim Stahl[2]
[1] AICES - RWTH Aachen University, Schinkelstraße 2, 52062 Aachen
[2] III Physikalisches Institut B, RWTH Aachen University, Otto-Blumenthal-Straße 52074 Aachen

E-mail: wittel@aices.rwth-aachen.de

Abstract:

A significant amount of nuclear fuel has been used both in civilian as well as in military applications of nuclear energy in the past decades. The resulting radioactive waste presents an important verification challenge. Several detection techniques can be employed for verifying declarations of nuclear waste repositories. In contrast to other measurement techniques, antineutrinos, produced by isotopes still present in the nuclear waste that undergo beta decay, e.g. strontium-90, would be capable of propagating through a significant amount of shielding material without being attenuated. Clearly, this posits considerable challenges for the detector design and realisation. The detection technology usually involves measuring scintillation light or Cherenkov radiation. For verification purposes, the directionality of the observed antineutrino events is crucial, for instance, when searching for potentially undeclared storage sites. In this paper, we investigate the prospect of utilising a new neutrino detection technique involving highly granular, imaging liquid argon detectors. This technology is presently developed and validated by the neutrino physics community. It offers the advantage of unprecedented precision in measuring (anti)neutrino energies, incidence directions, and would have a remarkable spatial resolution which is needed to filter out background events. In this work, we perform and discuss a preliminary feasibility study for employing this emergent type of (anti-)neutrino detectors in the context of nuclear waste verification efforts.

Keywords: spent nuclear fuel; safeguards; anti-neutrino applications; liquid argon detectors

1. Introduction

The nuclear fuel used to operate any type of fission reactor, for civilian, research and military use, has a finite lifetime. Once it reaches the point where it can no longer sustain a chain reaction inside the reactor core, i.e. it becomes *spent fuel*, it is removed and replaced by fresh fuel. Depending on the reactor type (light-water moderated, CANDU, etc.) and, more importantly, on the reactor operation, between one quarter and one third of the core is typically extracted every 12-18 months and replenished with fresh fuel.

The International Atomic Energy Agency (IAEA) [1] evaluated that the global cumulative amount of spent fuel was approximately 380,500 tonnes heavy metal at the end of 2014 [2]. Furthermore, based on the output of the 438 reactors in operation in 2014, the IAEA estimated that about 10,000 tonnes heavy metal of spent fuel is discharged every year from the nuclear power plants operated by the IAEA member states. This implies that, presently, more than 430,000 tonnes heavy metal of spent fuel are stored around the world. Moreover, due to the growing demand for clean energy, several countries like China, India, Russia are planning to increase their nuclear capacity which would in turn lead to a more rapid increase in the quantity of spent fuel than the IAEA estimate.

Besides the technical and societal-political challenges that must be overcome in order to safely store the large amount of produced spent fuel, the possibility that a fraction of it can be covertly diverted for producing nuclear weapons raises strong concerns and presents a clear necessity for safeguarding.

This paper discusses the need for safeguarding the spent nuclear fuel (SNF) in section 2. The existing monitoring techniques as well as the new technologies currently under scrutiny are overviewed in section 3. In section 4, we examine a specific detector concept: liquid-argon based time projection chambers for detecting anti-neutrinos emitted by the isotopes present in SNF. Lastly, section 5 outlines the feasibility study concerning the use of liquid-argon detectors currently undertaken by our group.

2. The Necessity of Safeguarding Spent Nuclear Fuel

The typical spent nuclear fuel composition depends on how the reactor was operated, specifically, on burnup. The table below shows the evaluated composition of SNF extracted from a light-water reactor considering a burnup of 50GWd/t heavy metal [3]:

Material	Relative amount
Uranium (< 1% ^{235}U, mostly ^{238}U)	93.4%
Fission products (^{129}I, ^{90}Sr, ^{135}Cs, etc.)	5.2%
Plutonium	1.2%
Minor actinides (^{237}Np, ^{241}Am, ^{243}Cm, etc.)	0.2%

Table 1: Typical isotopic composition of spent nuclear fuel [3]

In the first 100 years after being removed from the reactor, the dominant radioactivity of the SNF stems from the β-decaying fission products, thus being an abundant source of anti-neutrinos. While many isotopes have rather short half-lives (in the order of several hours or a few days), a few like ^{90}Sr ($T_{1/2}$ = 28.78a) and ^{137}Cs ($T_{1/2}$ = 30.17a) still contribute, even decades later. This is particularly relevant when considering long term spent fuel storage solutions.

In addition to its high radioactivity, the presence of plutonium, a key ingredient in the fabrication of nuclear weapons, in the spent fuel reinforces the necessity of safeguarding it. The Institute for Science and International Security [4] estimated that, at the end of 2014, the amount of irradiated (i.e. present in spent fuel) and unirradiated (directly usable for nuclear weapons) plutonium was approximately 2,400 tonnes [5]. A breakdown of the civil plutonium stocks per country at the end of 2014 is given in Fig.1.

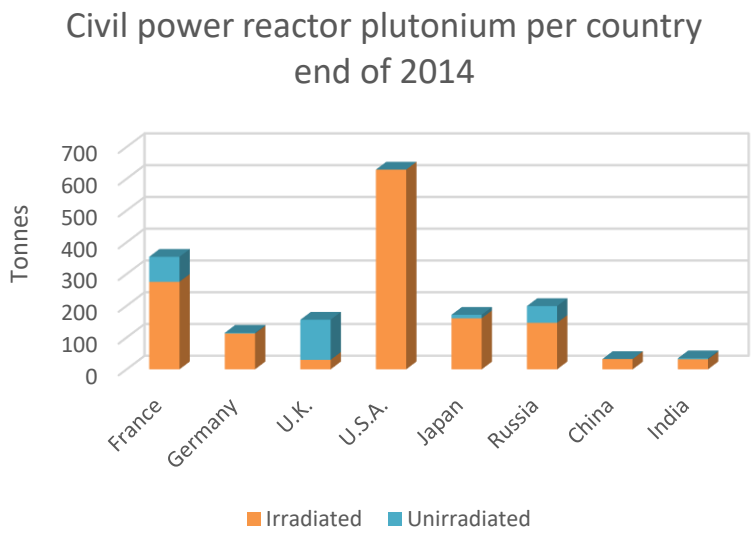

Figure 1: The amounts of irradiated and unirradiated plutonium held by country at the end of 2014. [5]

The IAEA current significant quantity definition for plutonium, i.e. the minimum amount of plutonium required for the construction of a nuclear weapon, is 8kg [6]. This implies that the quantity of irradiated and unirradiated plutonium at the end of 2014 would have been sufficient to produce 300,000 more

nuclear weapons. Furthermore, the Institute for Science and International Security evaluated that in the time period between 2004 and 2014, the plutonium stock has increased by a rate of approximately 50 tonnes per year.

The unirradiated plutonium is more susceptible for proliferation, since it can be readily used for nuclear weapons production. However, as can be seen in Fig. 1, a significantly larger amount of plutonium is found in spent fuel from where it can also be extracted through reprocessing techniques like e.g. PUREX, a process that separates the components based on their solubility in two different solutions. On a much smaller scale, plutonium can also be separated in hot cells, i.e. heavily shielded chambers with a controlled atmosphere where remotely manipulated devices can be used to work on radioactive materials.

Presently, civilian reprocessing facilities are operated in France, the United Kingdom, Japan, Russia and India. Approximately 2000 tonnes heavy metal of the total amount of produced spent fuel are reprocessed yearly [3]. The obtained uranium and plutonium are typically meant to be used for refuelling reactors. Nevertheless, safeguards are necessary to ensure that they are not diverted for weapons production.

3. Spent Nuclear Fuel Monitoring

Due to the considerable amount of decay heat and the high radiotoxicity, the spent fuel, once removed from the reactor, is immediately stored on-site, in water pools, for a cooling down period ranging from a few months to several decades. After the cooling down time, the SNF can be moved to wet or dry (air-cooled) storage facilities located either on the reactor site or in dedicated centralised repositories. From there, it can be either reprocessed or deposited in long-term geological storage.

The IAEA is presently monitoring the spent fuel during all the management stages in NPT non-nuclear-weapons states and, together with Euratom, in France and the United Kingdom, including their civilian SNF reprocessing programmes. In addition to on-site inspections, several technologies that provide continuous remote surveillance are deployed. This is crucial for providing the necessary continuity of knowledge, ensuring that no amount of fissile material obtained from SNF is diverted for weapons production. A brief overview of the technologies presently employed for this purpose is given in the following subsection [7] [8].

3.1 Current Monitoring Technologies

- **Camera surveillance system:** the cameras are placed in sealed containers (“tamper-indicating”) and are powered by long lasting batteries. The authenticity of the recorded data is ensured by three different levels of cryptographic security systems. The cameras are installed in storage areas and in the vicinity of spent fuel water pools and take images at time intervals between one second and ten minutes. Specialised software is then used to pre-scan the recorded images. Finally, inspectors evaluate the data and verify that it was consistent with the normal operation of the monitored facility.

- **Non-destructive assay systems:** consist of radiation detectors to measure gamma and neutron radiation and other sensors that monitor the temperature, etc. The data collected by these sensors are usually corroborated with the images taken by the surveillance cameras. In addition, a mobile unit neutron detector can be mounted onto the spent fuel casks to ensure that material is not removed from the cask during transportation.

- **Seals:** *(i)* single use metal cap seals, numbered and with unique markings on their inner surface, *(ii)* COBRA seals, containing a multicore optic fibre cable, *(iii)* electronic optical sealing system which can provide remote information and can be linked with the video surveillance system, *(iv)* laser mapping for containment verification.

3.2 Continuity of Knowledge

As the amount of spent fuel in storage accumulates, the probability that one of the monitoring techniques mentioned above may fail also increases with time. Should such a failure occur, especially in the case of cask seals, the contents of the affected casks can no longer be accounted for. While measuring the radiation that escapes from a cask with a damaged seal can demonstrate that its content is radioactive, it cannot provide enough information to determine if any amount of spent fuel is missing. Neutron or photon radiography techniques are also not feasible in this case due to the heavy shielding of the cask.

In order to verify the content of the cask and restore the continuity of knowledge, a tomographic technique based on cosmic muons was proposed and is currently under consideration [9]. The muons are produced when highly energetic astrophysical nuclei interact in the upper atmosphere and follow a broad energy distribution with the mean of approximately 4 GeV. Their average rate is of about 10^4 muons per minute and m^2 [9]. Muons can penetrate through significant amounts of material and provide important information about the cask's internal structure. Two tracking detectors, each consisting of several layers of drift-tubes, are placed on opposite sides of the cask. The tomographic information is obtained by measuring the muon attenuation [10], scattering [11] and associated particle production [12]. Thus, measurements of cosmic muons can be used as a stand-alone technique for verifying the contents of dry-storage casks.

A complementary approach, first proposed by P. Huber at al. [13], envisages measuring the anti-neutrino emissions coming directly from the spent fuel itself for long term monitoring and for ensuring continuity of knowledge. This application of anti-neutrino measurements, carried out in particular with liquid argon detectors, represents the main focus of this paper.

3.2 Anti-neutrinos as Potential Source of Information

As mentioned in section 2, the main source of radioactivity in the spent fuel comes from beta-decaying isotopes. The emitted anti-neutrinos can constitute a valuable source of information about the amount and content of the spent fuel in storage. Due to their weakly interacting nature, with cross-sections lower than 10^{-38} cm^2, they inevitably escape even large amounts of shielding. Clearly, this also implies that their detection raises considerable challenges which will be addressed later. In addition, since they are neutral particles, their travel directions are not modified by magnetic fields or by traversing matter. Thus, they can also provide direct information concerning the location of the SNF repository.

3.3. Characteristics of Anti-neutrinos from Spent Fuel

To evaluate the feasibility of using anti-neutrinos for measuring spent fuel, the characteristics of the emitted anti-neutrinos, i.e. the expected flux and energy range must be first considered.

This preliminary study relies on the anti-neutrino spectra calculations performed by P. Huber et al. [13]. For this purpose, a simulation of a pressurised-water Westinghouse reactor was implemented by the authors of [13] in the simulation code SCALE [14]. A fuel assembly configuration of 16×16 elements and an initial enrichment of 4% were assumed. The simulated reactor operation considered a burnup of 45GWd/t heavy metal [15].

The output of the simulation was the isotopic composition of the spent fuel at the time of discharge. This was considered the baseline. Making use of the ENSDF [16] decay data library, the beta-decay electron spectrum for each of the SNF isotopes was calculated at different points in time, e.g. 1 year, 10 years, etc, after being extracted from the reactor. The corresponding anti-neutrino spectra were then individually obtained by applying the conversion method, described for instance in [17].

The cumulative anti-neutrino spectra for 10, 30 and 50 years, respectively, after the spent fuel was discharged are illustrated in Fig. 2. As mentioned previously, after 10 years in storage, the main contributions to the anti-neutrino spectrum come from ^{90}Sr and ^{137}Cs. The discontinuities in the three spectra shown in Fig. 2 illustrate the fact that some isotopes decay in two stages: the first one characterised by a very small Q and, implicitly, a long lifetime, while the second is exactly the opposite [13]; here, Q represents the total energy released in the decay.

It is important to note the low energy of the anti-neutrinos coming from spent fuel: they are comparable to the solar neutrino spectra, as described in [18]. This constitutes additional challenges for the anti-neutrino detection.

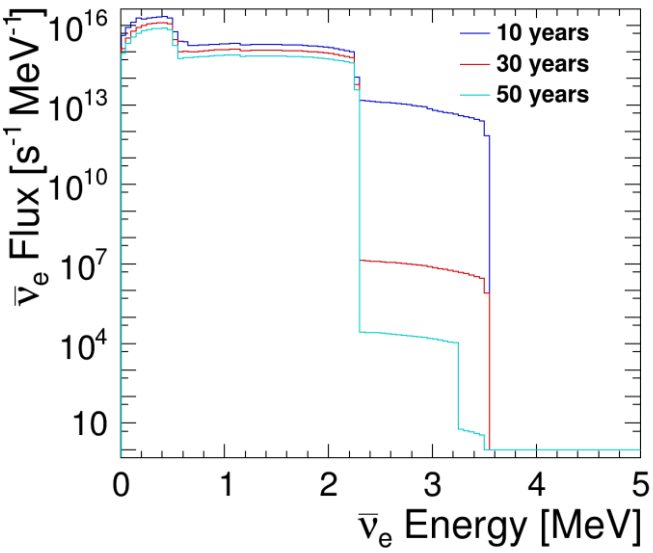

Figure 2: Energy spectra of anti-neutrinos emitted in the beta decays of isotopes present in the spent nuclear fuel. The figure was produced based on the calculations performed by P. Huber et al., [13]

3.4. Motivation for New Anti-Neutrino Detection Technologies in the Safeguards Context

The use of anti-neutrino measurements for monitoring purposes has already been considered in the case of nuclear reactors: for determining reactor shut-down periods or estimating the plutonium content in the core.

For instance, the WATCHMAN project [19] envisages an anti-neutrino detector containing 1810 tonnes of Gadolinium-doped water as sensitive material and an additional 1730 tonnes of the same material acting as a veto. The detector, in effect a cylindrical tank with a diameter and height of 15.8 metres, will be located in the Boulby mine in the United Kingdom and will measure anti-neutrinos coming from the Hartlepool two-reactor complex situated 25 km away. A similar project, called CHANDLER [20], proposes a smaller detector comprising up to 20 layers of 6 cm cubes of wavelength shifting plastic scintillator and thin sheets of lithium-6 (^{6}Li) loaded zinc sulfide (ZnS) scintillator.

In both WATCHMAN and CHANDLER detectors, the anti-neutrinos interact with the sensitive material by means of the so-called inverse beta decay (IBD) reaction: $\bar{\nu}_e + p \rightarrow e^+ + n$ (where the proton represents a hydrogen nucleus in water or plastic scintillator). The Cherenkov and scintillation light, respectively, produced as a result of an anti-neutrino interaction is read out by photomultiplier tubes in both detectors.

Since anti-neutrinos interact only weakly, the interaction target, i.e. the detector, must provide a large mass and a high density, such that the interaction rate is significant. The potential use water-Cherenkov detectors for spent fuel verification purposes may be limited especially by their size, e.g. 3.5 kT in the case of the WATCHMAN project.

An additional limitation stems from the energetic threshold of the inverse beta decay reaction itself, i.e. E_ν > 1.8 MeV. As can be seen from Fig. 2, this would essentially remove more than 80% of the anti-neutrinos emitted in beta-decays from spent fuel, thus significantly reducing the interaction probability. Consequently, a sensitive material which would enable anti-neutrino reactions without an intrinsic energetic threshold would be desirable.

Recently, as the interest in the field of fundamental neutrino research is gradually encompassing the energy range of solar and supernova anti-neutrinos, new detection methods are proposed and/or prototyped. In view of the spent fuel safeguarding requirements, anti-neutrino detectors based on liquid-

argon time-projection chambers (LArTPC) seem to be particularly promising. Such detectors have already been built and tested in experiments like, e.g. ArgoNeuT [21] and MicroBoone [22] and are considered for large-scale neutrino fundamental research experiments like DUNE [23].

4. Prospects for Safeguarding Spent Fuel with Liquid-Argon Detectors

The idea of using liquid-argon time projection chambers for neutrino detection was first proposed by Carlo Rubbia in 1977 [24]. It is only in the last decade that LArTPCs prototypes have been realised and tested. The working principles and advantages of this type of detectors are discussed in the following.

4.1. Fundamentals of Liquid-Argon Time Projection Chambers

A LArTPC consists of a large volume of liquid argon encompassed by a high-voltage cathode on one side and an anode on the opposite surface. In addition, several read-out wire planes are also located on the anode side. To be liquid, the argon must be cooled to a temperature of 87K (-186.15° C). The uniform electric field realised between the cathode and the anode planes typically has a strength of 500V/cm.

When an (anti-)neutrino interacts via charged or neutral current exchange with an argon atom, i.e. either with the orbital electrons or the nucleus itself, the emergent charged particles ionise and excite further argon atoms along their trajectory. The emitted free electrons drift in the liquid argon, under the force of the electric field, until they reach the read-out wires, in which they generate small currents. The wires are placed at very close distance to each-other, e.g. 3-5mm, and constitute a very dense net. To obtain multi-dimensional information about the charged particles' tracks, several wire planes can be used, placed under different angles with respect to each other.

In addition, the excited argon atoms also emit scintillation light in the ultraviolet range (λ=128nm) which can be measured with photosensors (PMTs). The light signal can provide highly useful timing information about the initial point of the anti-neutrino interaction and, implicitly, a way of determining its position along the drift trajectory. This is very useful in reconstructing a three-dimensional image of the charged particle's track.

4.2. Advantages of Liquid-Argon Anti-neutrino Detectors

The first benefit of using liquid-argon-based time projection chambers stems directly from their mode of operation: unlike water or scintillator detectors, they are *imaging* detectors - providing a three-dimensional reconstruction of the tracks left by the charged particles emerging from an anti-neutrino interaction. This is crucial for ensuring a good background rejection: in a safeguards context, the detectors will be deployed at the surface, i.e. without too much shielding from cosmic and cosmogenic background sources of neutrinos. The imaging properties of the LArTPCs ensure a very accurate energy reconstruction, based on the track length, and provide a means to infer the directionality of the incoming anti-neutrinos on an event-by-event basis. The SNF anti-neutrinos could be distinguished from the background using these two criteria.

The second advantage is the fact that argon (^{40}Ar) is in fact denser than both water and oil-based scintillator material. Having 18 protons (and electrons) and 22 neutrons, the number of targets for anti-neutrino interactions is higher in argon than in water, for instance, which has only 10 protons/electrons and 8 neutrons.

Furthermore, anti-neutrino interactions in argon produce two types of signal: the free electrons that drift and are collected on the read-out wires and the light emitted during the de-excitation of the argon atoms. In contrast, water or scintillator-based detectors provide only light as detection signal. In fact, liquid argon is an excellent scintillator, providing approximately 5000 photons/mm per minimum ionising particle.

Lastly, since argon constitutes approximately 1% of Earth's atmosphere, especially the ^{40}Ar isotope with an abundance of 99.6%, it is usually cheap to produce (and to liquify) and it is commercially available.

4.2. Relevant Interactions of Anti-Neutrinos in Liquid-Argon

In the standard water-Cherenkov or organic-scintillator-based detectors, (anti-)neutrinos mostly interact by means of the inverse beta decay process: $\bar{\nu}_e + p \rightarrow e^+ + n$. However, since there are no free protons available in liquid argon, this reaction cannot take place. Furthermore, as mentioned in section 3.4, its kinematic threshold of 1.8 MeV would severely limit the interaction rate of anti-neutrinos from spent fuel. The analogous reaction in liquid argon is the charged current absorption: $\bar{\nu}_e + {}^{40}\mathrm{Ar} \longrightarrow e^+ + {}^{40}\mathrm{Cl}^*$. However, its energy threshold in the case of anti-neutrinos is even higher: $E_\nu > 7.5$ MeV, which makes it unfeasible for SNF safeguarding (cf. Fig. 2).

Nevertheless, there are several other anti-neutrino interactions that may be helpful. The cross-sections of all the (anti-)neutrino interactions in liquid argon as well as other materials, for comparison, are summarised in Fig. 3.

- Neutral current excitation: $\bar{\nu}_e + {}^{40}\mathrm{Ar} \longrightarrow \bar{\nu}_e + {}^{40}\mathrm{Ar}^*$
  In this reaction, the excited argon atom would emit photons that could be measured by the photomultipliers.
- Elastic scattering: $\bar{\nu}_e + e^- \longrightarrow \bar{\nu}_e + e^-$
  The anti-neutrino scatters off electrons of the argon atoms. This reaction is very important for directionality and, implicitly, background rejection: the outgoing electron is scattered in the direction of the incoming anti-neutrino. However, the cross section of this interaction (blue line in Fig. 3) is rather low. In principle, it has no kinematic threshold, but there are limits to how small the energy of the emergent electron can be, i.e. it should be capable of leaving a measurable track in the detector. Based on a simple dE/dx calculation, we estimated that a 1 MeV scattered electron would leave a track with a length of approximately 1.4cm in a LArTPC. While this clearly posits a challenge for the read-out technology, these tracks are certainly not invisible in the detector. We are currently also investigating the feasibility of other potential read-out technologies.
- Coherent elastic neutrino-nucleus scattering:
  This interaction occurs via weak neutral current and essentially refers to anti-neutrinos being scattered off protons or entire nuclei. The cross-section of this reaction in liquid argon is presently being measure by experiments such as e.g. COHERENT [25]
  Despite the rather high cross-section (orange line in Fig. 3), the recoil energy is very low and it remains to be seen whether this reaction is detectable at all.

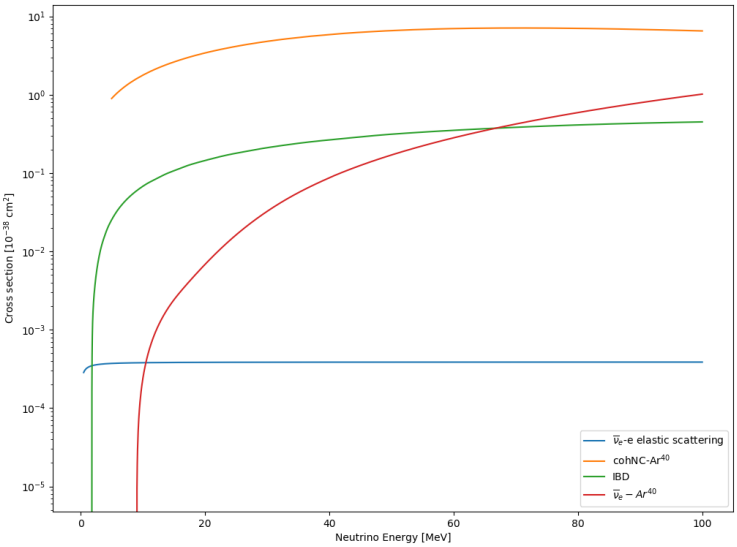

Figure 3: Cross-sections of anti-neutrino interactions in various materials. Figure based on SNOwGLoBES [26] cross section calculations.

4.3. Expected Event Rate

As a preliminary feasibility study, we have estimated the expected spent fuel anti-neutrino event rate in a liquid-argon time projection chamber and compared it with the rate expected in a water-Cherenkov detector of the same size. For this purpose, we assumed that both detectors have the standard volume of a shipping container, i.e. 80 m^3 [27], and that this entire volume is active and fully instrumented.

The event rate was calculated according to the known formula: $N_\nu(E_\nu) = \Phi_\nu(E_\nu) \cdot T \cdot \sigma(E_\nu)$, where Φ_ν is the energy dependent anti-neutrino flux, T is the number of targets in the detector active volume and σ is one of the relevant anti-neutrino differential cross-sections from Fig. 3.

For the LArTPC, we considered only the anti-neutrino-electron elastic scattering interaction (blue line in Fig. 3). Consequently, the number of *electron* targets present in the volume of liquid argon was computed with the formula: $T = (N_A \cdot \rho \cdot V)/M_W$, where N_A is Avogadro's number, ρ is the density of liquid argon, V is the detector active volume and M_W represents the molecular weight of argon. The anti-neutrino-electron elastic scattering differential cross-section was calculated by the authors of the SNOwGLoBES software package [26], based on [28].

In contrast, the inverse beta-decay reaction (green line in Fig. 3) was considered in the case of the water-Cherenkov detector and the number of *proton* targets was calculated in this case, similarly, for the same volume of ultra-pure water. The IBD differential cross-section was computed as mentioned previously, based on [29].

The anti-neutrino flux was determined based on the spent fuel anti-neutrino emission calculation carried out by P. Huber et al. [13] at time *t* = 10 years after discharge from the reactor core and assuming one tonne of spent fuel. A distance of 50 m between the detector and the SNF repository was taken into account in the $\bar{\nu}_e$flux calculation.

The estimated anti-neutrino event rates, both for liquid argon (black) and water-Cherenkov (red) detectors are shown in Fig. 4. While both detection technologies have very low event rates it can be seen that the rate in the water-Cherenkov detector can be up to 3 orders of magnitude larger. However, as mentioned previously in this section, the IBD reaction has the disadvantage of an energy threshold at 1.8 MeV; hence the shift in the starting point of the IBD (red) curve from Fig. 4.

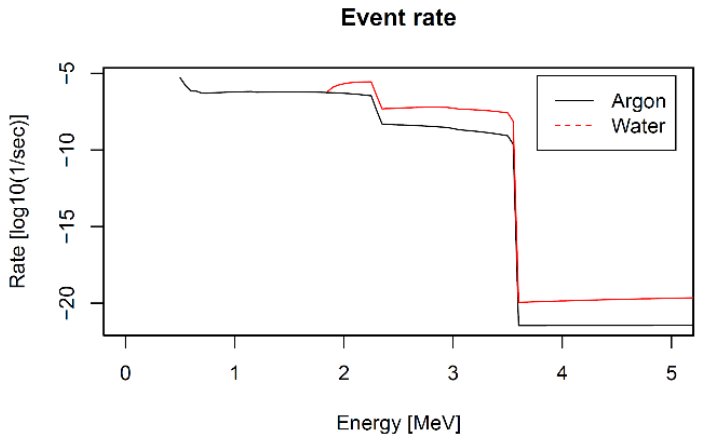

Figure 4: The estimated event rate in a LArTPC (black) and a water-Cherenkov (red) detector, respectively, with a volume of 80 m^3. This estimation assumes a 100% detector efficiency and only 1 tonne of SNF.

When comparing the event rate, integrated over the energy range between 0.5 and 3.2 MeV, the liquid argon and water-Cherenkov performance is very similar, with the former even slightly higher. This clearly indicates the limiting effect of the IBD energy threshold.

It must be noted that the shown anti-neutrino event rates represent an optimistic estimation, since this preliminary calculation assumes a 100% detector and background rejection efficiency.

5. Conclusions and Outlook

As the quantity of spent nuclear fuel increases worldwide, the risk of clandestine reprocessing activities with the specific purpose of diverting plutonium for nuclear weapons production informs the necessity of safeguarding known SNF repositories. Alongside cosmic muons that can traverse the shielding and content of the dry-storage casks, the only other messenger particles that could escape would be the anti-neutrinos emitted even decades later through the beta decays of isotopes like ^{90}Sr and ^{137}Cs still present in the spent fuel.

In this paper, we proposed the use of liquid-argon based time projection chambers for spent fuel monitoring. This technology is presently developed and validated by the neutrino physics community, thus aligning the nuclear verification efforts with the forefront of fundamental science. It presents several advantages in comparison to traditional detectors: (i) excellent track imaging capabilities – used for efficient background subtraction, (ii) a higher number of targets per unit volume which could somewhat compensate the lower reaction cross-sections, (iii) the emittance of two types of signal which enables three-dimensional track reconstruction and (iv) the relatively low production costs.

We performed a very preliminary calculation of the expected event rate in LArTPCs and compared it with the one achievable with a water-Cherenkov detector. Despite the significantly larger cross-section of the IBD reaction, the latter have the disadvantage of a relatively high energy threshold.

However, this estimate assumes perfect detector efficiency and background rejection. For a realistic feasibility study, the LArTPC performance should be studied in a full simulation that also takes the cosmic, cosmogenic and reactor background into account. This simulation together with a detailed treatment of the background form the subject of our future studies.

6. Acknowledgements

This work is funded by the Volkswagen Foundation through the “Freigeist” fellowship programme.

7. References

[1] IAEA - International Atomic Energy Agency, https://www.iaea.org/.

[2] International Atomic Energy Agency, *Nuclear Technology Review*, 2015. [Online]. Available: https://www.iaea.org/sites/default/files/ntr2015.pdf.

[3] International Panel on Fissile Materials, *Managing Spent Fuel from Nuclear Power Reactors*, 2011. [Online]. Available: http://fissilematerials.org/library/rr10.pdf.

[4] Institute for Science and International Security, www.isis-online.org/.

[5] D. Albright, S. Kelleher-Vergantini, D. Schnur, *Plutonium and Highly Enriched Uranium Inventories*, Institute for Science and International Security, 2015.

[6] International Atomic Energy Agency, *The Present Status of IAEA Safeguards on Nuclear Fuel Cycle Facilities*; IAEA BULLETIN- VOL.22, NO.3/4, [Online]. Available: https://www.iaea.org/sites/default/files/publications/magazines/bulletin/bull22-3/223_403400240.pdf.

[7] International Atomic Energy Agency, https://www.iaea.org/topics/safeguards-and-verification.

[8] International Atomic Energy Agency, https://www.iaea.org/newscenter/news/surveying-safeguarded-material-24/7.

[9] J.M. Durham et al., *Verification of Spent Nuclear Fuel in Sealed Dry Storage Casks via Measurements of Cosmic-Ray Muon Scattering*, Phys. Rev. App., vol. 9, p. 044013, 2018.

[10] J. Marteau et al., *DIAPHANE: muon tomography applied to volcanoes, civil engineering, archaelogy*, Journal of Instrumentation, vol. 12, p. C02008, 2017.

[11] K. N. Borozdin et al., *Surveillance: Radiographic imaging with cosmic ray muons*, Nature, vol. 422, p. 277, 2003.

[12] E. Guardincerri et al., *Detecting special nuclear material using muon-induced neutron emission*, Nucl. Instrum. Methods Phys. Res., vol. A, n. 789, p. 109, 2015.

[13] V. Brdar, P. Huber, J. Kopp, *Antineutrino Monitoring of Spent Nuclear Fuel*, Phys. Rev. Applied, vol. 8, DOI: 10.1103/PhysRevApplied.8.054050, 2017.

[14] SCALE, Oak Ridge National Laboratory, https://www.ornl.gov/scale.

[15] P. Huber, *private communication.*

[16] Evaluated Nuclear Structure Data File» [Online]. Available: https://nucleus.iaea.org/Pages/evaluated-nuclear-structure-data-file.aspx.

[17] A. C. Hayes and P. Vogel, *Reactor Neutrino Spectra*, 2016. [Online]. Available: https://arxiv.org/abs/1605.02047v1.

[18] K. Nakamura - The Particle Data Group, *Solar Neutrinos*, 2002. [Online]. Available: http://pdg.lbl.gov/2002/solarnu_s005313.pdf.

[19] M. Askins et al., *The Physics and Nuclear Nonproliferation Goals of WATCHMAN: A WAter CHerenkov Monitor for ANtineutrinos*, 2015, arXiv:1502.01132v1.

[20] The CHANDLER Detector Project , http://cnp.phys.vt.edu/chandler/.

[21] C. Anderson et al., *The ArgoNeuT Detector in the NuMI Low-Energy beam line at Fermilab*, 2012. [Online]. Available: https://arxiv.org/abs/1205.6747.

[22] R. Acciarri et al.- The MicroBooNE Collaboration, *Design and Construction of the MicroBooNE Detector*, 2017. [Online]. Available: https://arxiv.org/abs/1612.05824.

[23] The DUNE Collaboration, https://www.fnal.gov/pub/science/lbnf-dune/index.html

[24] C. Rubbia, *The liquid-argon time projection chamber: a new concept for neutrino detectors*, 1977. [Online]. Available: https://cds.cern.ch/record/117852?ln=en.

[25] The COHERENT Collaboration, https://sites.duke.edu/coherent/.

[26] SNOwGLoBES: SuperNova Observatories with GLoBES, http://webhome.phy.duke.edu/~schol/snowglobes/.

[27] International Organization for Standardization, «ISO 668:2013 - Series 1 freight containers - Classification, dimensions and ratings,» 2013. [Online]. Available: https://www.iso.org/standard/59673.html.

[28] Z. P. William J Marciano, *Neutrino–electron scattering theory*, Journal Phys. G, vol. 29, DOI:10.1088/0954-3899/29/11/013, 2003.

[29] F. V. Alessandro Strumia, *Precise quasielastic neutrino/nucleon cross section*, Phys. Lett. B, vol. 564, DOI:10.1016/S0370-2693(03)00616-6, 2003.